JOURNAL OF MATERIALS SCIENCE **38** (2003) 1517– 1521

Characterization of Ti-Al-Er alloy produced via direct laser deposition

C. A. BRICE*‡, H. L. FRASER
Department of Materials Science and Engineering, The Ohio State University, Columbus, OH 43210, USA
E-mail: craig.a.brice@lmco.com

Recent advances in manufacturing technology have led to the development of a new breed of advanced materials. These new materials are process dependent and would be difficult, if not impossible, to produce using conventional methods. Laser direct manufacturing (LDM) is a solid freeform fabrication process that enables the production of these advanced materials. LDM utilizes a high energy density heat source, powdered metal feedstock, and computer driven machine controls to produce bulk materials in near-net shape form. The combination of powdered metallurgy (P/M) and rapid solidification processing (RSP) allow bulk structures to be made with novel compositions and unique properties. In addition, near-net shape production eliminates the need for thermomechanical post-processing that can nullify some of the metallurgical advantages gained through RSP and P/M. These advantages have led to the development of alloys specifically tailored to the LDM process. This paper describes a dispersion hardened erbium-bearing titanium alloy developed to couple with the processing advantages found in the laser direct manufacturing process.

1. Introduction

Laser direct manufacturing (LDM) is a process that has recently gained much attention [1–4]. Three main hardware components are required for the LDM process: a laser heat source (typically Nd: YAG or CO_2), a powdered metal delivery system, and a computer driven motion control system. Fig. 1 shows a schematic of the basic setup. The first step is to create a three-dimensional model of the object to be deposited. After slicing the computer model into discrete layers and rows, a path is generated and loaded into the motion control computer. These motion controls then drive the workhead and/or work table to trace out the computer generated path. The laser is focused onto a substrate, creating a molten pool. As powdered metal is carried into the focus area, a semi-continuous weld-bead deposit is created. These weld beads overlap as the deposition progresses, resulting in a fully dense, near-net shape object produced directly from a three-dimensional computer file.

The potential benefits in terms of cost and time-to-product savings make this process attractive for a number of industrial applications. Parts can be produced near-net shape, reducing or eliminating the need for machining or thermomechanical processing. The LDM process also reduces the need for expensive molds, dies, and forging blanks, thus saving considerable time and money. Furthermore, the additive nature of the process greatly reduces scrap material. Excess powder is easily recovered and reused. All of these advantages make this process ideal for rapidly producing complex shapes that are traditionally forged or machined from blanks.

In addition to process benefits, the LDM technique can also be used to achieve unique metallurgical structures and properties. Alloying of normally insoluble elements is possible through the inherent rapid solidification processive (RSP) characteristic. Metastable phases can be formed that are difficult to achieve using conventional processing methods. Powdered metal materials can be alloyed *in situ*, forming composite and/or graded materials with unique properties. And through careful atmosphere control, it is possible to alloy monitored levels of interstitial elements with the deposited material. These metallurgical benefits are applicable to a wide range of alloy systems, thus creating a class of alloys specific to the LDM process.

This paper discusses one such LDM-specific alloy, Ti-8Al-1Er. Erbium has been added to conventional titanium alloys for oxygen gettering [5] and for dispersion hardening in splat quenched alloys [6–9]. RSP behavior allows the erbium to be supersaturated in the titanium matrix and subsequently precipitated out of solution as very fine, homogeneously distributed erbium-bearing particles. These particles significantly strengthen the material by interfering with dislocation motion. Unfortunately, splat quenching proved

*Author to whom all correspondence should be addressed.
‡Currently at Lockheed Martin Aeronautics Company, Fort Worth, TX 76108.

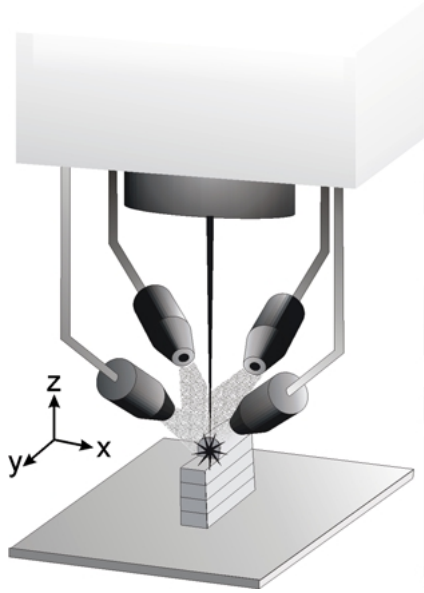

Figure 1 Schematic of laser deposition process. Powder is carried by argon out of the nozzles and is fused into a solid deposit by the laser.

impractical because of the consolidation operation that is required to form a bulk part from powder. The LDM process, however, allows for the production of this same alloy without the need for consolidation or other post-production treatments. In addition to erbium, eight weight percent aluminum was added for substitutional solid solution strengthening and alpha phase stabilization, which is necessary for elevated temperature microstructural stability. Interstitial solid solution strengthening was also achieved by absorption of gaseous elements (oxygen, nitrogen) from the atmosphere.

2. Experimental

Pre-alloyed Ti-8Al-1Er powder was obtained from Crucible Research, Pittsburgh, PA. The powder was gas atomized in argon, then screened to give a size distribution of −80/+200 mesh. This powder was used to deposit test samples in the LDM processing facility located at Lockheed Martin Aeronautics Company, Fort Worth, TX. Bulk samples 1.3 cm by 1.3 cm by 2.5 cm were deposited with a laser power of 425 W and a travel speed of 50.8 cm/min. In addition, thin wall samples were deposited using a single bead helical structure (2.5 cm radius) with 300 W power and 30.5 cm/min travel speed. All samples were deposited onto a 0.6 cm Ti-6Al-4V substrate contained inside an argon-filled processing chamber maintained at 760 torr.

Three heat treatments were carried out on the samples for comparison with the as-deposited condition. Sections were encapsulated in quartz, evacuated, and backfilled with 20 kPa argon. These samples were subjected to the following heat treatment: (1) stress relief anneal −30 minutes at 540°C, (2) full anneal −2 hours at 700°C, and (3) long term anneal −100 hours at 700°C. The as-deposited and heat treated samples were then sectioned and prepared for examination. Scanning electron microscopy (SEM) samples were mounted in conductive phenolic, polished, and etched using Kroll's Reagent. Transmission electron microscopy (TEM) samples were core drilled and sliced using electrodischarge machining, then thinned using a combination of jet electropolishing and ion milling. Small sections from each sample were sent to Anderson Laboratories, Greendale, WI, for complete chemical analysis.

3. Results and discussion

A linear single pass structure was deposited to establish a baseline in the microstructural development of the rapidly solidified material. This isolated the as-deposited microstructure and eliminated thermal effects encountered during the deposition of adjacent beads. The single pass microstructure consists of acicular α' martensite with a small number of nanoscaled second phase particles located at the grain boundaries

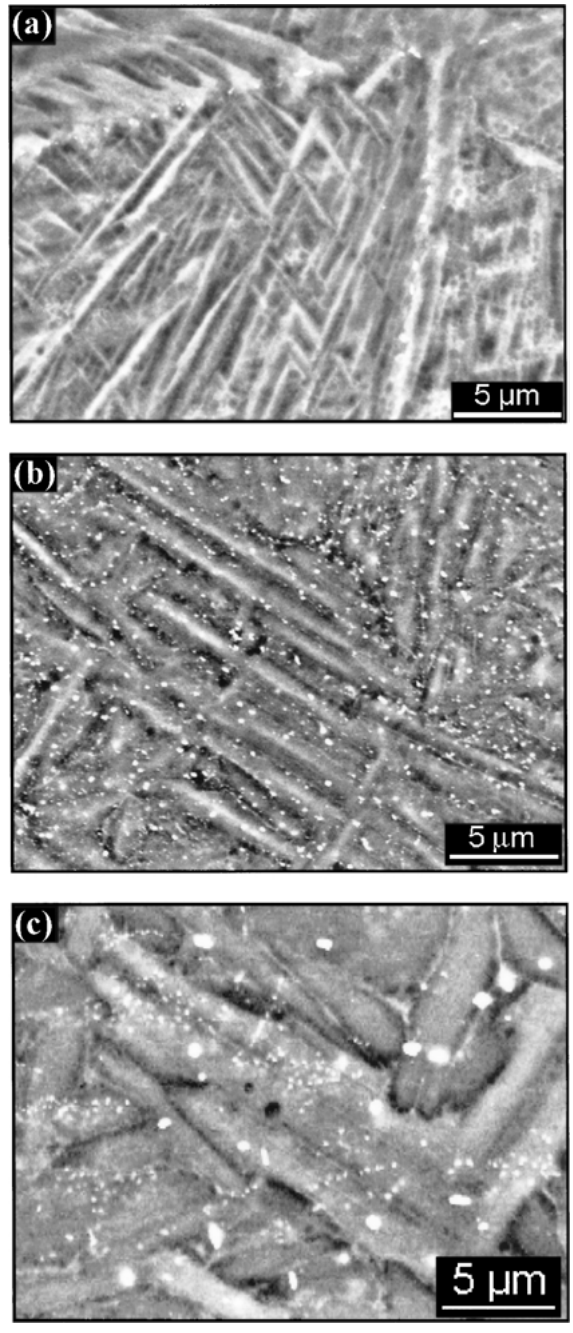

Figure 2 Backscattered electron SEM micrographs of (a) single bead deposit, (b) bulk deposit, and (c) thin wall deposit. Note the lack of second phase in the single pass deposit. Multiple passes of the laser precipitate out erbium dispersoids in the bulk and thin-wall deposits.

(Fig. 2a). These particles are likely erbium or erbium compounds, however, analysis was not performed to verify the exact second phase chemistry. Nonetheless, it is evident that much of the erbium remains in solid solution, thus creating a metastable, supersaturated microstructure.

Multiple pass structures were then deposited in order to examine the effect of thermal cycling on the single pass metastable structure. The multiple-pass bulk structure, shown in Fig. 2b, shows a very fine, homogeneously distributed second phase that was precipitated out of the as-deposited supersaturated solid solution. A higher volume fraction of erbium-bearing particles is evident in this microstructure. The thermal cycling encountered in the deposition of multiple rows and layers effectively heat treats adjacent beads *in situ*. As subsequent layers are deposited, the previous layers are heated to a temperature high enough to precipitate the erbium out of solution. The precipitates are spherical in shape and generally range from 50 to 100 nanometers in diameter.

The thin wall deposit exhibits a bimodal distribution of particles as seen in Fig. 2c. The smaller particles are similar in size and shape to the precipitates in the bulk deposit. The larger particles are also spherical and approximately 500 nanometers in diameter. The development of these large particles is influenced by the geometry controlled cooling behavior of the thin wall structure. The single pass structure is no more than one millimeter wide, essentially constricting the heat flow through the deposit to two dimensions. This two-dimensional heat flow reduces the cooling rate of the solidified metal through the beta phase field ($T_\beta \cong 980^\circ$C). In titanium, the beta phase is a non-close packed body-centered cubic (bcc) structure, thus coarsening occurs much more rapidly in this phase than in the hexagonal close-packed (hcp) phase. Reducing the cooling rate by restricting the heat flow to two dimensions allows the deposit to remain in the beta region longer, resulting in coarsening of the erbium-bearing compounds.

Further evidence of heat flow dependent precipitation behavior is shown in Fig. 3. This SEM micrograph shows bands of higher density precipitation coinciding with bands of internal macroporosity. The pores interrupt the heat flow through the deposit and create local hot spots within the structure. These hot spots retard the cooling rate and thus allow the adjacent matrix more time in the beta region. The result is increased diffusion of erbium upon solidification and an increase in erbium-bearing precipitates after thermal cycling.

TEM examination of the particles revealed that precipitation occurs at dislocations and grain/lath boundaries (Fig. 4). In the as-deposited structure, erbium particles segregate to defects in the lattice. Thermal cycling from subsequent deposition layers allows interstitial elements to diffuse to the erbium particles at the defects and form erbium compounds. These erbium compounds were identified using electron diffraction in the TEM. A small precipitate was isolated in the thin region of a TEM foil. The sample was tilted to a zone allowing a clear spot pattern to be obtained. Comparison of the experimental pattern with a simulated pattern revealed the structure of the particles to be consistent with that of Er_2O_3 (Fig. 5).

Several heat treatments were carried out on the samples to investigate the stability of the erbium oxide dispersion. Very little microstructural change was seen in the heat treated samples. Within each group, bulk or thin wall, the only visible difference was a slight coarsening of the alpha lath structure. Fig. 6 shows SEM micrographs comparing the as-deposited bulk sample and the same bulk sample after 100 hours at 700°C. It is apparent from the micrographs that no coarsening occurred after long term elevated temperature exposure.

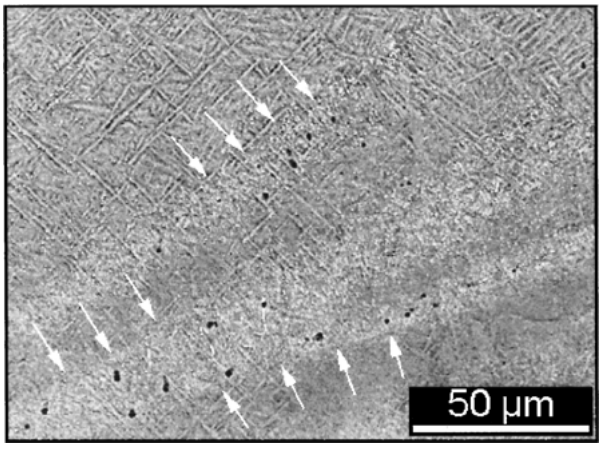

Figure 3 Backscattered electron SEM micrograph showing bands of increased precipitate density corresponding with bands of macroporosity.

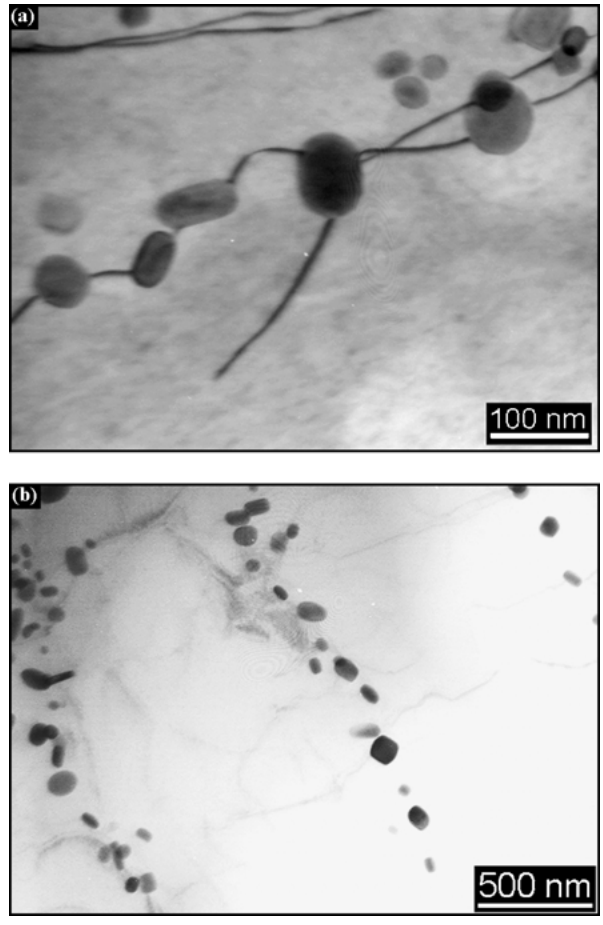

Figure 4 Brightfield TEM micrographs showing (a) precipitate formation along dislocations and (b) along lath boundaries.

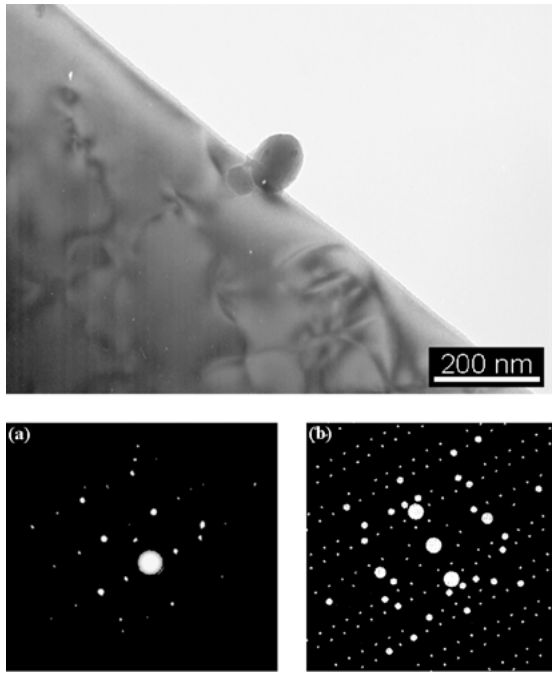

Figure 5 Brightfield TEM micrograph showing particle on thin region of foil and (a) experimental and (b) simulated selected area diffraction pattern along the [112] zone of Er_2O_3.

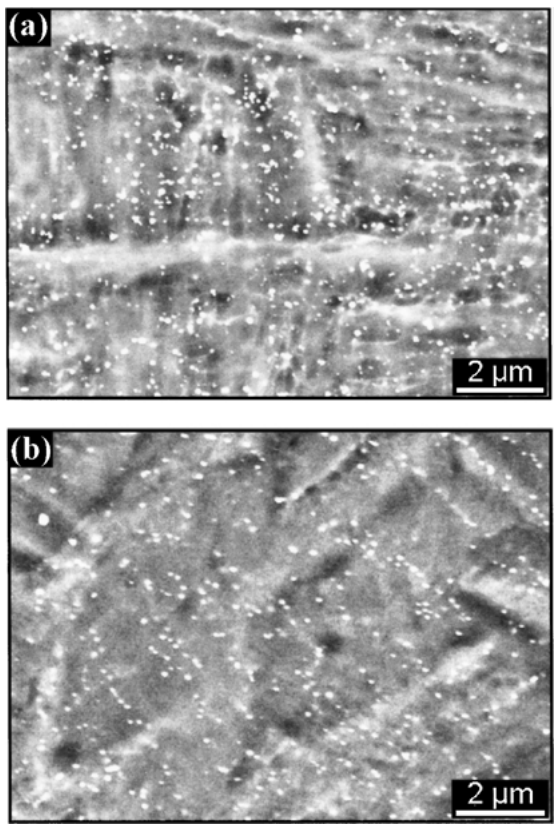

Figure 6 Backscattered electron SEM micrographs of (a) bulk Ti-8Al-1Er microstructure as-deposited and (b) bulk microstructure after 100 hours at 700°C. Note the lack of precipitate coarsening.

This thermodynamic stability of the microstructure has been shown to be dependent on an excess amount of dissolved oxygen in the lattice [10]. Chemical analysis was performed on samples from each heat treatment to compare interstitial levels. Fig. 7 shows a graph comparing the interstitial levels from the four heat treatments. Oxygen levels were about 2.5 times higher than

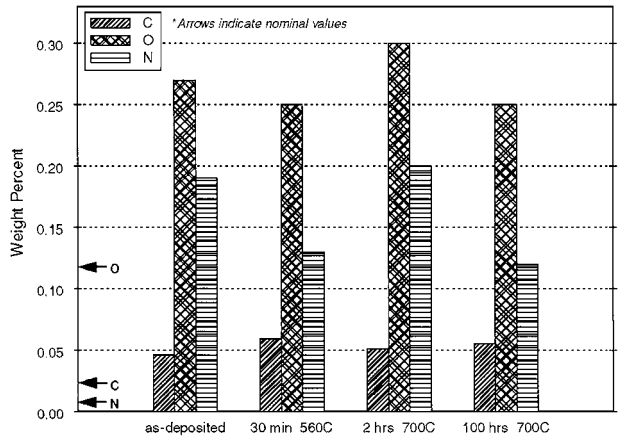

Figure 7 Results of chemical analysis on laser deposited Ti-8Al-1Er test specimens. Note nominal interstitial values indicated by arrows along the vertical axis.

the nominal value of 0.115 wt% provided by the powder supplier. Nitrogen levels exceeded 20 times the nominal value. This contamination was likely due to gaseous absorption during the deposition process. Tighter atmosphere controls are needed to lower the interstitial elements to reasonable levels and eliminate potential embrittlement.

Comparison of the bulk versus thin wall specimens indicated a distinct difference in the precipitation behavior in 100 hour exposure samples. Fig. 8 shows

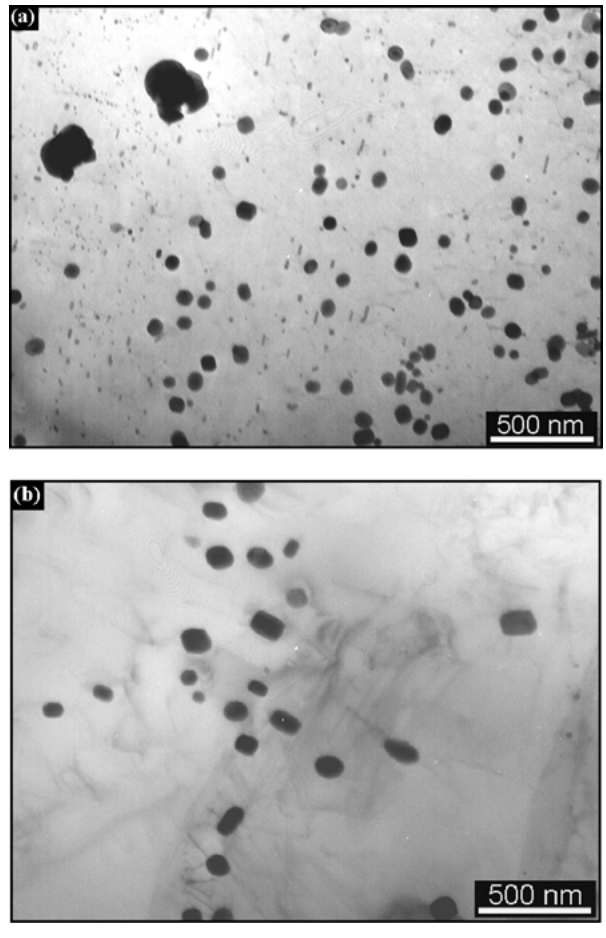

Figure 8 Brightfield TEM micrographs showing (a) the bulk sample after 100 hours at 700°C and (b) the thin wall sample after the same heat treatment. Note the lack of any further precipitation in the thin wall structure.

representative TEM micrographs from both the bulk and thin wall long term anneal specimens. The bulk sample shows evidence of further precipitation of erbium oxide while the thin wall sample does not. This suggests that the slower cooling rate in the thin wall specimens allows all of the erbium to react with oxygen during cooling, leaving no erbium available for subsequent precipitation upon heat treatment. Conversely, the faster cooling rates in the bulk material allow some erbium to be retained in solid solution that can then be precipitated out during heat treatment.

4. Conclusions

Laser direct manufacturing technology was used to produce bulk and thin wall deposits of Ti-8Al-1Er. The deposits exhibited a fine, homogeneous dispersion of Er_2O_3 particles in an acicular α' matrix. The bulk deposits showed a fine distribution of 50 to 100 nanometer particles, while the thin wall deposits had a bimodal distribution with some particles in the 500 nanometer range. Both structures were stable at elevated temperatures, however, the bulk sample showed signs of continued precipitation upon heat treatment while the thin wall structure did not. Heat flow through the structure determines the microstructure that is developed. Restricted heat flow can produce larger precipitates and/or a higher density of precipitates. Excess interstitial content is likely due to atmosphere contamination during the deposition process.

Acknowledgments

Funding for this work was provided by Lockheed Martin Corporation, Bethesda, MD. Special thanks to Ken Cluck at Lockheed Martin for providing the as-deposited samples and to Su Meng at The Ohio State University for her help with TEM sample preparation.

References

1. D. M. KEICHER, *Metal Powder Report* **55**(9) (2000) 32.
2. C. L. ATWOOD *et al.*, in Proc. ICALEO '98, Laser Materials Processing Conf., Orlando, FL, Nov 1998 (Laser Institute of America, 1998).
3. D. M. KEICHER and J. M. SMUGERESKY, *JOM* **49**(5) (1997) 51.
4. E. SCHLIENGER *et al.*, in Proc. of 3rd Pacific Rim Intl. Conf. on Adv. Mat. and Proc. (1998).
5. B. B. RATH *et al.*, in Proc. 4th Intl. Conf. on Titanium (1980) Vol. 2, p. 1185.
6. S. M. L. SASTRY, T. C. PENG, P. J. MESCHTER and J. E. O'NEAL, *JOM* **35**(9) (1983) 21.
7. S. H. WHANG, *ibid.* **36**(4) (1984) 34.
8. S. M. L. SASTRY, P. J. MESCHTER and J. E. O'NEAL, *Met. Trans.* A **15A**(7) (1984) 1451.
9. S. M. L. SASTRY, T. C. PENG and L. P. BECKERMAN, *ibid.* **15A**(7) (1984) 1465.
10. D. G. KONITZER, R. KIRCHHEIM and H. L. FRASER, *Rapidly Solidified Metastable Materials* **28** (1984) 345.

Received 13 February
and accepted 27 December 2002